Chemosphere 201 (2018) 370–379

Contents lists available at ScienceDirect

Chemosphere

journal homepage: www.elsevier.com/locate/chemosphere

4-Chlorophenol degradation using ultrasound/peroxymonosulfate/nanoscale zero valent iron: Reusability, identification of degradation intermediates and potential application for real wastewater

Gelavizh Barzegar [a], Sahand Jorfi [b], Vahid Zarezade [c], Masoumeh Khatebasreh [d], Fayyaz Mehdipour [e], Farshid Ghanbari [f, *]

[a] Department of Environmental Health Engineering, Behbahan Faculty of Medical Sciences, Behbahan, Iran
[b] Environmental Technologies Research Center, Ahvaz Jundishapur University of Medical Sciences, Ahvaz, Iran
[c] Behbahan Faculty of Medical Sciences, Behbahan, Iran
[d] Environmental Science and Technology Research Center, Department of Environmental Health Engineering, Shahid Sadoughi University of Medical Sciences, Yazd, Iran
[e] Department of Environmental Health Engineering, School of Public Health, Shahid Beheshti University of Medical Sciences, Tehran, Iran
[f] Department of Environmental Health Engineering, Abadan School of Medical Sciences, Abadan, Iran

HIGHLIGHTS

- nZVI was synthesized and its function was investigated on PMS activation.
- nZVI/PMS/US was effective to degrade 4-CP.
- Simultaneous application of nZVI and US boosted PMS activation and 4-CP degradation.
- Intermediates of 4-CP degradation were also determined.
- The performance of nZVI/PMS/US was evaluated on petrochemical wastewater treatment.

GRAPHICAL ABSTRACT

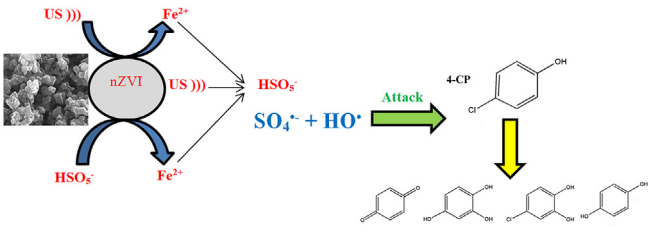

ARTICLE INFO

Article history:
Received 6 December 2017
Received in revised form
31 January 2018
Accepted 23 February 2018
Available online 27 February 2018

Handling Editor: Jun Huang

Keywords:
Peroxymonosulfate
Ultrasound
Intermediates
nZVI
4-Chlorophenol

ABSTRACT

In this study, nanoscale-zero valent iron (nZVI) was synthesized and its function was assessed in ultrasound (US)/peroxymonosulfate (PMS)/nZVI process to degrade 4-chlorphenol (4-CP). The influential operation parameters of US/PMS/nZVI were evaluated on 4-CP degradation. 95% of 4-CP was degraded during 30 min under the conditions of pH = 3.0, nZVI = 0.4 g/L, PMS = 1.25 mM, US power = 200 W. The rate constants of 4-CP degradation for US/PMS/nZVI, PMS/nZVI, US/PMS and US/nZVI were 0.1159, 0.03, 0.0134 and 0.0088 min^{-1} respectively. Simultaneous application of US and nZVI synergistically increased 4-CP degradation and PMS activation. nZVI was compared with Fe^{2+}, Fe^{3+} and micro-ZVI and their results indicated high performance of nZVI compared to others. Reusability of nZVI was examined in four cycles. nZVI exhibited that reusability was acceptable in three runs. The results of effect of anions showed that phosphate had significant inhibitory effect on 4-CP degradation in US/PMS/nZVI process. The scavenging experiments indicated that hydroxyl radical had more contribution compared to sulfate radical. Intermediates of 4-CP degradation were identified including five aromatic compounds. Reaction pathway of 4-CP degradation was proposed. Finally, the performance of US/PMS/nZVI process was

* Corresponding author.
E-mail address: Ghanbari.env@gmail.com (F. Ghanbari).

https://doi.org/10.1016/j.chemosphere.2018.02.143

evaluated on real petrochemical wastewater. The results showed that US/PMS/nZVI can be a suitable pretreatment for biological treatment.

1. Introduction

Treatment of wastewaters had been always met different challenges to reach required standards or new rules. These challenges are now increasing especially in wastewaters containing toxic and recalcitrant organic pollutants. Conventional methods usually are ineffective for complete degradation of these pollutants. 4-Chlorophenol (4-CP) is one of the most important derives of phenol group which has strong resistance to chemical and biological remediation (Elghniji et al., 2014; Moonsiri et al., 2004). 4-CP can seriously threaten living organisms including human beings. The acceptable daily intake (ADI) of 4-CP is estimated 0.1 mg/kg body weight per day. 4-CP is generally found in industrial wastewaters such as pulp and paper wastewater, petrochemical wastewater and effluent of pesticide manufacture. Toxicity and non-biodegradability of 4-CP have prompted many scientists to study the chemical oxidation of 4-CP (Czaplicka, 2004; Moonsiri et al., 2004; Theurich et al., 1996; Tong et al., 1997). Advanced oxidation processes (AOPs) have exhibited high efficiency in degradation of refractory organic compounds. These processes are well-known as the processes generating the hydroxyl radical (Mahamuni and Adewuyi, 2010; Vilar et al., 2017). Many AOPs have been conducted on 4-CP degradation including Fenton oxidation (Zhou et al., 2008), direct and catalytic ozonation (Sauleda and Brillas, 2001), photocatalysis (Lettmann et al., 2001) and electrochemical oxidation (Johnson et al., 1999). Nowadays, sulfate radical-based AOPs (SR-AOPs) have received a great attention by the scientists for degradation of environmental pollutants in contaminated water and wastewater (Ghanbari and Moradi, 2017). Sulfate radical ($SO_4^{\bullet-}$) is a strong and powerful oxidant with redox potential of 2.5–3.1 V (Neta et al., 1988; Pan et al., 2017; Yao et al., 2017). Recently, peroxymonosulfate (HSO_5^-) (PMS) has exhibited successful function to generate sulfate radical for degradation of organics (Ghanbari and Moradi, 2017). PMS can be activated by transition metals (homogenous and heterogeneous forms) (Ahmadi et al., 2017; Huang et al., 2017), ultraviolet (He et al., 2013), ultrasound (Su et al., 2012) and free-metal heterogeneous catalysts (Sun et al., 2014). Although cobalt has exhibited high performance for PMS activation, iron is a benign element and non-toxic. Hence, most studies have focused on iron-based catalysts. Zero valent iron (ZVI) has long shown promise for effectively activating hydrogen peroxide as Fenton-like process (Yazdanbakhsh et al., 2015). Nanoscale-ZVI (nZVI) has demonstrated the high performance in water and wastewater treatments in different roles. nZVI not only is a reducing agent, but also it is a source of ferrous ions for activating PMS (Hussain et al., 2012). In this way, nZVI can generate Fe^{2+} in the presence of PMS based on following equations.

$$Fe \rightarrow Fe^{2+} + 2e^- \quad (1)$$

$$Fe + HSO_5^- + 2H^+ \rightarrow Fe^{2+} + HSO_4^- + H_2O \quad (2)$$

The generated Fe^{2+} consequently actives PMS to produce sulfate radicals through Eq. (3) (Anipsitakis and Dionysiou, 2004).

$$Fe^{2+} + HSO_5^- \rightarrow Fe^{3+} + SO_4^{\bullet-} + OH^- \quad (3)$$

Besides, many researchers have combined transition metal with ultrasound (US) to improve degradation efficiency. In this way, US activates PMS to generate both sulfate and hydroxyl radicals according to Eq. (4) (Ghanbari and Moradi, 2017; Su et al., 2012).

$$HSO_5^- +))) \rightarrow SO_4^{\bullet-} + OH^{\bullet} \quad (4)$$

Moreover, US also increases corrosion of nZVI to generate the ferrous ion based on Eq. (5) (Yuan et al., 2016).

$$Fe +))) \rightarrow Fe^{2+} + 2e^- \quad (5)$$

In fact, the combination of US, nZVI and PMS probably enhances the generation rate of free radicals and accelerates the degradation of organic pollutants. Based on literature, nZVI/persulfate ($S_2O_8^{2-}$) and nZVI/H_2O_2 have been widely studied on the degradation of phenol-based compounds (Dong et al., 2017; Li et al., 2015; Xu and Wang, 2011). Moreover, PS/US/nZVI and H_2O_2/US/nZVI processes have been used for the degradation of organic pollutants (Taha and Ibrahim, 2014; Zou et al., 2014). To the best of our knowledge, a few researches have been focused on PMS/nZVI for degradation of organic pollutants. In addition, the process of US/PMS/nZVI has not been studied on 4-CP degradation yet. In this study, we synthesized nZVI by a facile method and investigated the catalytic activity of nZVI in the presence of US for the activation of PMS to degrade 4-CP in aqueous solution. Moreover, several key operation parameters (nZVI dosage, PMS dosage, pH, reaction time and US power) were investigated on 4-CP degradation. Mineralization, mechanism, the effect of some anions and reusability were also studied. Finally intermediates of 4-CP degradation were identified and the performance of US/PMS/nZVI was evaluated on real wastewater.

2. Materials and methods

2.1. Chemicals

All chemicals and reagents were in analytical grade. 4-chlorophenol (4-(Cl)C_6H_5OH) was purchased from Merck Company with purity of 99%<. Oxone salt ($KHSO_5.0.5KHSO_4.0.5K_2SO_4$) as PMS source and sodium phosphate (Na_3PO_4) were purchased from Sigma-Aldrich. Sodium chloride (NaCl) and sodium sulfate (Na_2SO_4), were provided from Dr.Mojaalli Company (Iran). Hydrogen peroxide (30%), potassium hydroxide and sulfuric acid (98%) were obtained from Merck Company. Ferric chloride hexahydrate ($FeCl_3.6H_2O$), was purchased from BDH Inc. Sodium borohydride (98%<), was purchased from Sigma-Aldrich Company. Potassium ferricyanide and 4-aminoantipyrine were purchased from Daejung Chemicals. Water and methanol (HPLC grade) were purchased from Samchun Company. Petrochemical wastewater was collected from petrochemical industry which was located in Mahshahr city (Iran) as the biggest industry of petroleum in Iran. The samples were kept in temperature 4 °C.

2.2. Preparation of nZVI

nZVI particles were synthesized based on the reduction of iron ion (Liou et al., 2006; Wang and Zhang, 1997; Yuan et al., 2016). Accordingly, 0.25 M $FeCl_3.6H_2O$ aqueous solution was introduced to a beaker. Then, 0.4 M $NaBH_4$ aqueous solution as reducing agent

was dropwisely added with flow rate (10 mL/min) under N_2 atmosphere. After 60 min mixing, black precipitations were formed and they were separated by a Nd_2Fe1_4B magnet. The precipitations were washed three times with absolute ethanol and then dried in the vacuum condition. The morphology and particle size were analyzed by field emission scanning electron microscope (FESEM) (Mira 3-Xmu). The integrated energy-dispersive X-ray spectroscopy (EDS) was used to determine the elements in fresh and reused nZVI. Crystallographic structure of nZVI was determined by X-ray diffraction (XRD) analysis which was recorded by a D8 Bruker advanced diffractometer with Cu-Kα radiation (40 kV and 40 mA). The magnetism of nZVI was analyzed by vibrating sample magnetometer (VSM-MDK-Iran).

2.3. US/PMS/nZVI experiments

All experiments were conducted in a cylindrical reactor made of Plexi-glass with diameter of 6 cm and height of 12 cm. 300 mL of 25 mg/L 4-CP was introduced to the reactor, then a known amount of nZVI was added to the solution. A certain concentration of PMS was injected to the solution. Sonication was carried out by a Q125 ultrasonic generator (400 W, 20 kHz) equipped with a probe transducer made of titanium. The sonication probe was immersed at the solution (3 cm under the water surface). The amplitude of sonication was adjusted at 100% in which sonication was performed continuously. The pH solution was adjusted by KOH and H_2SO_4 with concentration of 0.1 M. At given reaction time intervals, samples (4 mL) were taken out and then immediately quenched with 2 mL methanol and then filtrated by syringe filters (0.22 microne). The temperature was fixed by water jacket at 27–31 °C during sonolysis reaction. In each reusability experiment, the nZVI was separated using a Nd_2Fe1_4B magnet and washed thoroughly with deionized water. The experiments were carried out at least in duplicate and the analyses of parameters were conducted in triplicate. The average values were used in the results.

2.4. Analytical methods

The concentration of 4-CP was determined by using a KNAUER HPLC (High Performance Liquid Chromatography) equipped with a 2500 ultraviolet (UV) detector at $\lambda = 278$ nm and C18 column (250 mm × 4.6 mm, with 5 μm particle size) was employed for the separation as the stationary phase. The isocratic mobile phase was methanol and water with 30:70 ratio at a flow rate of 1.0 mL/min. The 20 μL was manually injected while the column temperature was set at 25 °C. Total organic carbon (TOC) values were measured by a TOC analyzer (Shimadzu). Chemical oxygen demand (COD), total dissolved solids (TDS), 5-days biochemical oxygen demand (BOD) were analyzed based on Standard Method (APHA, 1999). The iron concentrations were measured by an atomic absorption spectrometer (Analytik Jena, Vario 6). PMS was determined according to iodometric titration method (Vogel, 1989). Total phenols were determined based on colorimetric method by a spectrophotometer (Hach DR6000) at 500 nm according to the reaction of phenol compounds with 4-aminoantipyrine (APHA, 1999). Liquid chromatography mass spectroscopy (LC-MS) analysis was applied to recognize the intermediates of 4-CP degradation using by a Micromass Quattro Micro API mass spectrometer (Waters 2695., Milford, MA). Chromatographic separation was achieved on a C18 column (50 mm × 2.1 mm id, 1.7 μm; Waters) at 25 °C. The MS was operated in negative mode with electrospray source ionization, by applying an interface voltage of −4.5 kV. The mobile phase was methanol and water which was modified by 0.1% acetic acid and 20 mM ammonium acetate in which the flow rate was 1 mL/min. The injection volume of the sample was 25 μL.

3. Results and discussion

3.1. nZVI characteristics

Fig. 1a and b shows the FESEM images of nZVI. As shown in Fig. 1a, generally, the nanoparticles were sphere-like shape and they were agglomerated which could be due to the magnetical interactions between each of the nano-ZVI. The FESEM image with high magnification (Fig. 1b) demonstrates that the size of nanoparticles is in range of 20–80 nm. Fig. 1c presents the EDS spectrum of nZVI. The spectrum showed that the elements of synthesized nZVI were consisted of Fe (84.3% wt) and O (11.2% wt) indicating that nZVI was partially oxidized before reaction time. Fig. 1e shows XRD spectrum of synthesized nZVI. A sharp peak at $2\theta = 44.80°$ corresponded to (110) plane confirmed the formation of Fe^0. Moreover, two peaks of $2\theta = 65.27°$ and $2\theta = 82.56°$ which were

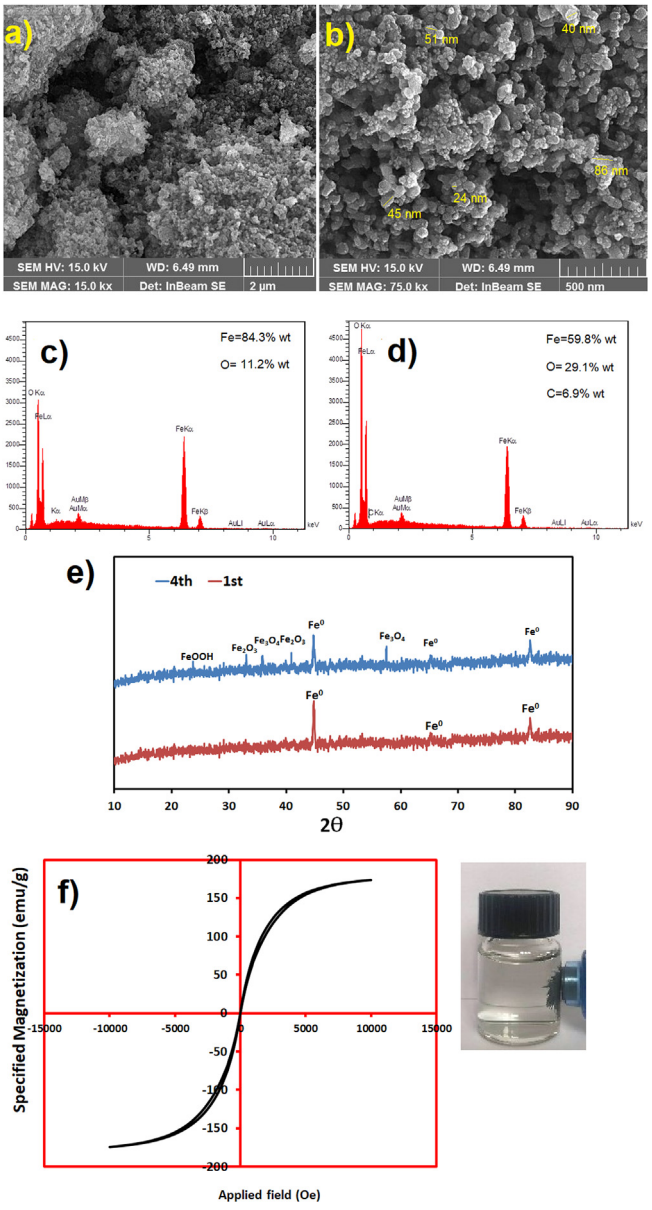

Fig. 1. (a) and (b) FESEM images of nZVI (c) EDS spectrum of fresh nZVI (d) EDS spectrum of nZVI after 4th cycle use (e) XRD spectrum of nZVI before and after reaction (f) magnetization hysteresis loop of nZVI.

respectively corresponded to planes of (200) and (211) were related to Fe^0. It should be noted that a small peak was observed at $2\theta = 33.08°$ which was related to Fe_2O_3 confirming the oxidation of Fe^0 by air before reaction. Fig. 1f displays the magnetization hysteresis loop of nZVI. The saturation magnetization (Ms) was found to be 164 emu/g indicating that nZVI can be easily separated by a small magnet from aqueous solution.

3.2. The effect of key operational parameters (pH, nZVI dosage, PMS dosage, ultrasound power)

The solution pH is a critical factor affecting the performance of the US/PMS/nZVI process in the degradation of contaminants due to its function in control of the activity of the free radicals, the catalytic activity, and iron species. Fig. 2a shows the effect of pH on 4-CP degradation in US/PMS/nZVI process under the conditions of 1 mM PMS, 0.4 g/L nZVI, 200 W ultrasound power and 30 min reaction time. As can be seen, with increase of pH, the degradation of 4-CP was dramatically reduced. The acidic condition increased the release of ferrous ion from the surface of nZVI resulting in the more activation of PMS. In the presence of high proton, nZVI was corroded and ferrous ions were provided for PMS activation to generate sulfate radicals. At pH of 2.0 and 3.0, 4-CP degradation was about 75% while this value reached 38.3% at pH = 7.0. The reducing the removal efficiency was related to the precipitation of iron species at pH > 4. The species of iron hydroxides deactivate nZVI through the precipitation of $Fe(OH)_n$ and $Fe(OH)^{(n-1)+}$ (Babuponnusami and Muthukumar, 2012; Zha et al., 2014). Moreover, it is worthwhile to emphasize that the power of free radicals in acidic condition is more than that in alkaline condition (Burbano et al., 2005). Therefore, pH = 3.0 was suitable for 4-CP degradation in US/PMS/nZVI process.

The effect of nZVI dosage was investigated in range of 0.1–0.5 g/L under the condition of pH = 3.0, 1 mM PMS, 200 W ultrasound and 30 min reaction and their results are shown in Fig. 2b. Increase of nZVI dosage generally enhanced the generation of free radicals through catalyzing PMS. Based on Eq. (3), increase of ferrous ion boosted generating the sulfate radicals, therefore, degradation of 4-CP was consequently increased. Accordingly, 4-CP removal efficiencies were 45.1, 58.3, 75, 86.5 and 79.4% for 0.1, 0.2, 0.3, 0.4 and 0.5 g/L respectively. Results showed that the removal efficiency was decreased in 0.5 g/L nZVI indicating that higher dosage of nZVI did not favor for PMS activation (Ahmadi et al., 2017). In fact, higher dosage of nZVI as well as ferrous ions scavenged sulfate and hydroxyl radicals and produced non-reactive anions (Eq. (6)) (Wang and Chu, 2012). Hence, the dosage of 0.4 g/L nZVI was the best dosage for PMS activation.

$$Fe^{2+} + (SO_4^{\bullet-} \text{ or } HO^{\bullet}) \rightarrow Fe^{3+} + (SO_4^{2-} \text{ or } OH^-) \quad (6)$$

PMS dosage is the main factor for the production of sulfate and hydroxyl radicals, in other words, PMS is the main source of sulfate and hydroxyl radicals. Herein, the effect of PMS dosage was evaluated on 4-CP degradation under conditions of pH = 3.0, 0.4 g/L nZVI, 200 W ultrasound power and related results are illustrated in Fig. 2c. Regarding the results, by rising the PMS dosage from 0.5 to 1.25 mM, 4-CP degradation was linearly increased in a way that 4-CP removals were 35.1, 68.6, 86.5 and 95% for 0.5, 0.75, 1 and 1.25 mM respectively. Generally, increase in PMS dosage leads to more generation of sulfate radicals. However, it has been reported in literature that higher PMS concentration has negative effect on the concentration of sulfate and hydroxyl radicals. In current work, at 1.5 mM PMS, degradation efficiency of 4-CP was dropped to 90.3%. Excessive PMS can scavenge both sulfate and hydroxyl radicals and decrease the removal efficiency. In these reactions, peroxymonosulfate radical was produced which was ignored in degradation of organic pollutants due to low potential redox ($E^0 = 1.1$ V) (Jaafarzadeh et al., 2017; Ling et al., 2010).

$$HSO_5^- + SO_4^{\bullet-} \rightarrow SO_4^{2-} + SO_5^{\bullet-} + H^+ \quad (7)$$

$$HSO_5^- + HO^{\bullet} \rightarrow SO_5^{\bullet-} + H_2O \quad (8)$$

The effect of ultrasound power was investigated in three levels (100, 200 and 300 W) (Fig. 2d). As clearly observed, the degradation of 4-CP was increased from 74.6% to 95% when ultrasound power was raised from 100 W to 200 W. This increase can be related to the fast regeneration of Fe^{2+} at the solution improving the cycle of forming the free radicals. In US power of 300 W, no significant increase in 4-CP degradation was observed indicating that 200 W US

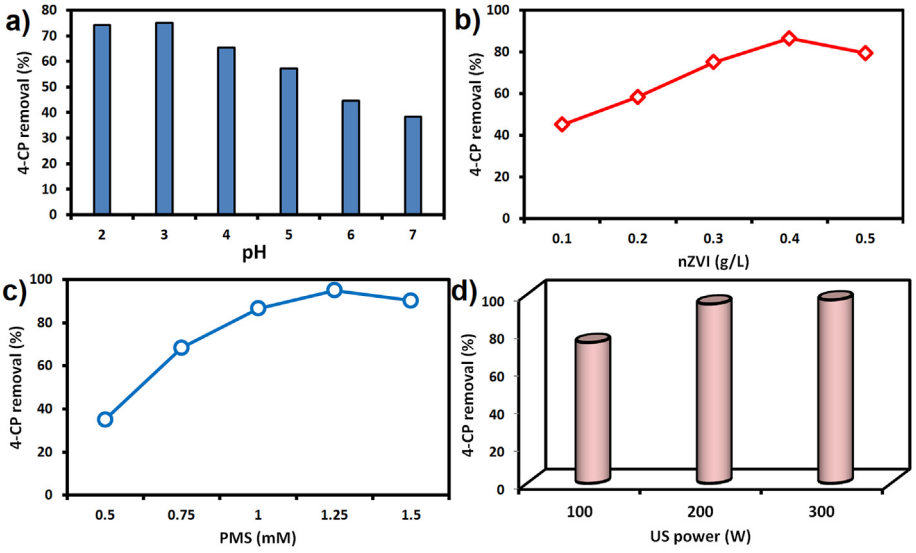

Fig. 2. (a) the effect of pH on 4-CP removal (PMS = 1.0 mM, US power = 200 W, nZVI = 0.4 g/L and 30 min) (b) the effect of nZVI dosage on 4-CP removal (PMS = 1.0 mM, US power = 200 W, pH = 3.0 and 30 min) (c) the effect of PMS dosage on 4-CP removal (nZVI = 0.4 g/L, US power = 200 W, pH = 3.0 and 30 min) (d) the effect of US power on 4-CP removal (nZVI = 0.4 g/L, PMS = 1.25 mM, pH = 3.0 and 30 min).

power was sufficient for activation of PMS and regeneration of iron species. It is worthwhile to emphasize that an increase in temperature (32–37 °C) occurred at 300 W US power which can enhance PMS activation through thermolytic cleavage of O–O bond. In fact, in higher power in sono-based process, heat activation of oxidants can be a promoter method for the generation of free radicals.

3.3. The role of nZVI and US in PMS activation

Various processes were evaluated to determine the role of nZVI and US in PMS activation. Fig. 3a shows the 4-CP removal in different processes. As clearly observed, the removal efficiency of 4-CP was negligible when only PMS was used. This showed that no free radicals were produced during reaction. On the other hands, lone application of nZVI and US removed 16 and 12% of 4-CP respectively. nZVI is able to adsorb of 4-CP and it also may eliminate 4-CP based on reductive dechlorination. The few free radicals were produced in lone US application whose concentrations were insufficient for 4-CP degradation. In binary systems, removal efficiency was reasonably improved. PMS/US degraded 31.6% of 4-CP within 30 min reaction time. Based on Eq. (4), high energy of US decomposed PMS to hydroxyl and sulfate radicals. However, this activation was ineffective in 30 min reaction time. 57.9% of 4-CP was omitted in the silent system of PMS/nZVI. Compare to US, nZVI showed a higher catalytic activity for PMS activation. Homogeneous reactivity of PMS with ferrous ion generated is high; therefore, sulfate radicals were significantly produced in the solution. In the main system (US/PMS/nZVI), 4-CP degradation efficiency was obtained 95% in 30 min indicating synergistic effect of the concurrent presence of nZVI and US for PMS activation. In this way, not only US irradiation can accelerate Fe^{2+} generation from nZVI, but it can also clean the surface of nZVI. In fact, US irradiation prevented deactivation of nZVI. Moreover, $H^{\bullet}$ produced from Eq. (4) may activate PMS based on Eq. (9). On the other hand, hydrogen radical may react with sulfate radicals to generate sulfate ions (Eq. (10)).

$$HSO_5^- + H^{\bullet} \rightarrow SO_4^{\bullet-} + H_2O \quad (9)$$

$$SO_4^{\bullet-} + H^{\bullet} \rightarrow HSO_4^- \quad (10)$$

In order to confirm the synergistic effect of US and nZVI, PMS was monitored during reaction time in different systems. Fig. 3b shows the trend of PMS reduction in various conditions. As can be seen, the decrease in PMS concentration in lone PMS application was poor while US and nZVI could decompose 30% and 46% of PMS during 30 min reaction time respectively. These results confirmed that nZVI was more successful than US in terms of PMS activation. In the presence of US and ZVI, PMS was considerably decomposed in a way that 77% of PMS is reduced during 30 min reaction time. The results showed that the presence of both activators synergistically activated PMS to produce free radicals. The rate constants (k, min^{-1}) of PMS and 4-CP decays were determined by pseudo first-order model ($\ln C/C_0 = -kt$). Synergistic effect (SE) of the presence of both activators can be quantified for PMS decay and 4-CP degradation based on Eqs. (11) and (12).

$$SE_{4-CP} = \frac{k_{US/PMS/nZVI}}{k_{PMS/nZVI} + k_{US/nZVI} + k_{US/PMS}} \quad (11)$$

$$SE_{PMS} = \frac{k_{US/PMS/nZVI}}{k_{PMS/nZVI} + k_{US/PMS}} \quad (12)$$

The rate constant of 4-CP degradation for US/PMS/nZVI, PMS/nZVI, US/PMS and US/nZVI were 0.1159, 0.03, 0.0134 and 0.0088 min^{-1} respectively. Based on Eq. (11), the SE value of 4-CP degradation for US/PMS/nZVI was obtained 2.2 (more than 1) indicating that both activators had synergistic effect on 4-CP degradation. In case of PMS decay, SE value was obtained 1.6. These results proved that US can affect the nZVI through two mechanisms; increase of Fe^{2+} generation and cleaning the surface of ZVI.

Dissolved iron (DI) was measured during reaction time in different conditions to confirm the synergistic effect of US/PMS/nZVI. Fig. 4 shows the DI in nZVI-based systems. As can be seen, DI was increased at first 10 min in all systems. After that, the DI concentration was gradually dropped within reaction time. DI concentration in US/PMS/nZVI reached 34.3 mg/L at 10 min while DI concentrations respectively were 18.9 and 15.6 mg/L for PMS/nZVI and US/nZVI at the same time. These results showed that PMS and US increased the ferrous ion generation significantly. Compared to

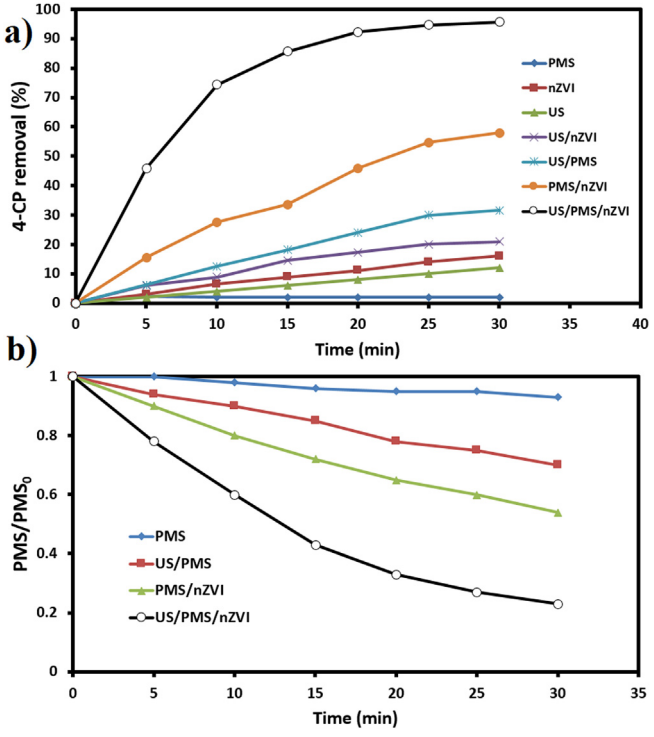

Fig. 3. (a) the 4-CP removal in different processes (b) PMS decay in different conditions (nZVI = 0.4 g/L, PMS = 1.25 mM, pH = 3.0 and US power = 200 W).

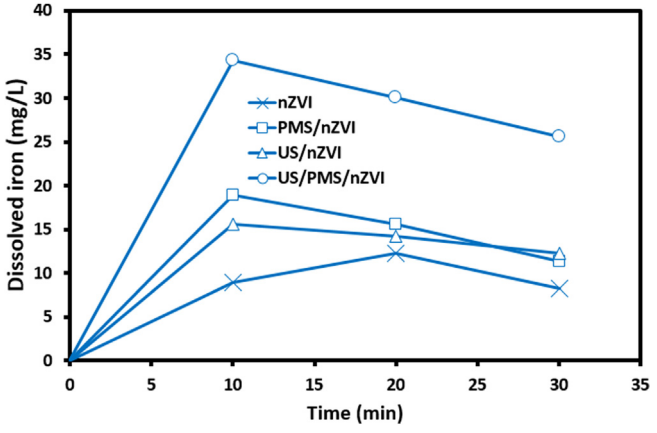

Fig. 4. the dissolved iron concentration in different processes (nZVI = 0.4 g/L, PMS = 1.25 mM, pH = 3.0 and US power = 200 W).

the sole application of nZVI, US/nZVI and PMS/nZVI released more ferrous ion to the solution. However, after 10 min, the DI was dropped which was related to the precipitation of iron in forms of hydroxide. In fact, when Fe^{2+} was released to the solution, it affected the solution pH and induced the precipitation of iron species. DI concentration in US/PMS/nZVI was 25.6 mg/L at 30 min reaction time which was still considerable amount for PMS activation. US and PMS were effective to maintain the desirable amount of Fe^{2+} in the solution.

3.4. The comparison with Fe(II), Fe(III) and micro-Fe^0

The performance of nZVI in PMS/US/catalyst system was compared with micro-Fe^0 (mZVI) and ferrous and ferric ions and their results are presented in Fig. 5. As can be seen, in homogeneous systems (US/PMS/Fe(II) and US/PMS/Fe(III)), 4-CP degradation was increased at the first 15 min and after that reached steady state within 30 min reaction. It seems that available iron ions were rapidly consumed at the first 15 min to activate PMS. The regeneration of iron from iron complexes was slow in the homogenous systems. Whereas, in mZVI and nZVI systems, 4-CP degradation was gradually increased during 60 min reaction time which was attributed to continuous release of iron ion to the solution. However, nano-scale ZVI exhibited high performance compared to micro-scale ZVI. As expected, nZVI had the higher activity for the surface reactions and ferrous generation in comparison with mZVI. It should be noted that nZVI profits both heterogeneity and homogeneity behavior in catalytic activation of PMS. Moreover, US can regenerate ferrous ion and clean the surface of nZVI to produce more iron (Adewuyi, 2005a, b). Based on the results obtained, nZVI showed high performance in ferrous ion generation and PMS activation.

3.5. The reusability of nZVI

The reusability of nZVI in US/PMS/nZVI process was evaluated in fourth cycle for 4-CP degradation and related results are presented in Fig. 6a. As observed, increasing the number of recycle run declined the degradation rate of 4-CP considerably. In this way, the degradation efficiency of 4-CP was decreased from 95.6% to 73.5% at 4th cycle. This decrease in the efficiency can be related to the deactivation of the surface of nZVI for ferrous ion generation. Indeed, the surface of nZVI was poisoned by the intermediates of 4-CP or the precipitation of iron species. This phenomenon can reduce the releasing the ferrous ion into the solution. However, the degradation efficiency of 4-CP was acceptable after three cycle (85% removal efficiency). In order to confirm the reducing ferrous ion generation in the consequent experiments, dissolved iron was measured during four cycles and their results are illustrated in Fig. 6b. As shown, the trend of DI was the same in all recycling runs of nZVI. Howbeit, the DI was decreased by consequent recycling of nZVI in which DI concentration of 34.3 mg/L in fresh use reached 18.2 mg/L at 4th run. In fact, the corrosion at the surface of nZVI reduced due to poisoning the nZVI as above-mentioned. In order to confirm this issue, nZVI after 4th run was analyzed by EDS (Fig. 1d). As can be seen, the weight percent of iron was decreased from 84.3% (in fresh mZVI) to 59.8% (in 4th run) indicating that iron content was decreased through the leaching of ferrous ion. Besides, the weight percent of oxygen was increased from 11.2% to 29.1% for 4th run which was attributed to the oxidation of nZVI by oxidative agents such PMS and free radicals. Moreover, EDS spectrum showed carbon element (6.9% wt) which might be related to the adsorption of 4-CP and its intermediates on the surface of nZVI. It should be noted that EDS analysis was conducted at 4th cycle of nZVI. Hence, the accumulation of organic compounds could occur during 4 cycles of nZVI. The oxidation of the surface of nZVI was determined by XRD analysis after 4th run (Fig. 1e). As can be seen, different iron oxides were formed on the surface of nZVI including Fe_2O_3, Fe_3O_4

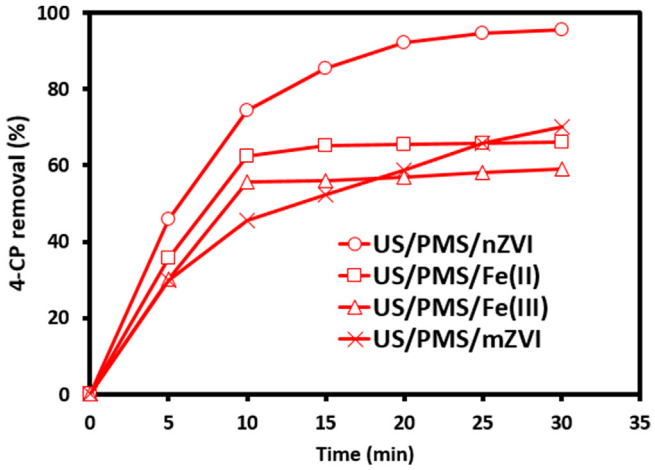

Fig. 5. 4-CP removal in different systems (mZVI = nZVI = 0.4 g/L, PMS = 1.25 mM, pH = 3.0, US power = 200 W and Fe(II) = Fe(III) = 1 mM).

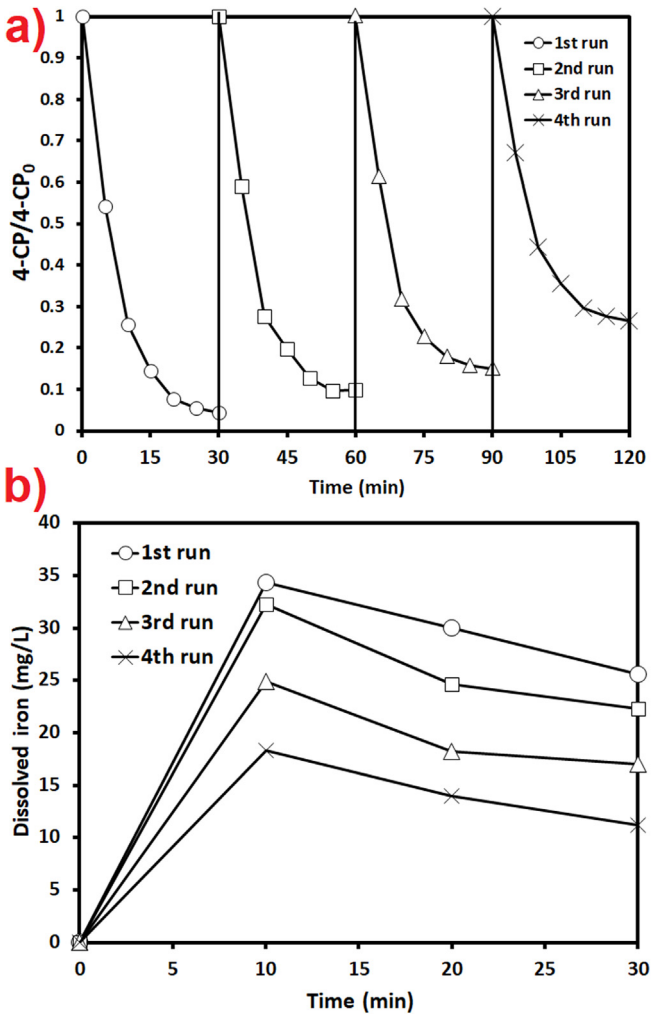

Fig. 6. the reusability of nZVI in four cycles (a) 4-CP degradation (b) DI during reaction time (nZVI = 0.4 g/L, PMS = 1.25 mM, pH = 3.0 and US power = 200 W).

and FeOOH. These results confirmed that nZVI after 3th run maintained catalytic activity for PMS decomposition.

3.6. The effect of sulfate, chloride and phosphate

In free radical-based processes for water and wastewater treatment, anions can affect the efficiency of the process through scavenging the free radicals. The effects of chloride, phosphate and sulfate anions in different concentrations were evaluated on 4-CP degradation in US/PMS/nZVI process. Fig. 7a presents the 4-CP removal in the presence of chloride ion. As can be seen, the presence of 1 mM Cl^- improved the degradation of 4-CP slightly. The chloride ion can increase the corrosion of nZVI and enhance consequently ferrous ion concentration in the solution resulting in more activation of PMS (Devlin and Allin, 2005; Hernandez et al., 2004). With increase of the concentration of Cl^- (5 and 10 mM), the 4-CP degradation was reduced. Although chloride ion increased nZVI corrosion, the chloride ion could scavenge sulfate and hydroxyl radicals significantly and produced the chlorine species with lower redox potential (Chan and Chu, 2009; Wang et al., 2011). In fact, chloride ion had a bilateral role in US/PMS/nZVI process in which its high concentration played an inhibition role for 4-CP degradation.

Fig. 7b shows the effect of sulfate ion on 4-CP degradation in US/PMS/nZVI process. As can be seen, in the presence of 1 and 5 mM sulfate ion, no change in performance of US/PMS/nZVI process was observed while a small reduction occurred in the presence of 10 mM sulfate ion. Since inherent mechanism of US/PMS/nZVI is based on sulfate radical, the presence of sulfate ion did not affect the free radicals. However, the increase in ionic intensity (10 mM sulfate ion) can be a logical reason for inconsiderable reduction of 4-CP degradation (Jaafarzadeh et al., 2017).

Fig. 7c depicts the effect of the phosphate ions on 4-CP degradation in US/PMS/nZVI process. As shown, increase in phosphate ion concentration increased the inhibition effect on 4-CP degradation. This inhibition effect was significant in the presence of 10 mM phosphate ions. Phosphate ions influenced the 4-CP degradation in US/PMS/nZVI process through three mechanisms. First, phosphate ions are attached to the surface of nZVI and reduce the catalytic activity (Qi et al., 2014). Second, phosphate ions react with ferrous ion generated and $Fe_3(PO_4)_2$ is formed with $Ksp = 1 \times 10^{-36}$ which are easily precipitated. Indeed, phosphate competes with PMS for reaction with iron (Wilfert et al., 2015). Third, phosphate ions can scavenge free radicals as well as other anions (X^-) and produce the weaker radical based on Eq. (13).

$$(SO_4^{\bullet-} \text{ or } HO^{\bullet}) + X^- \rightarrow (SO_4^{2-} \text{ or } HO^-) + X^{\bullet} \quad (13)$$

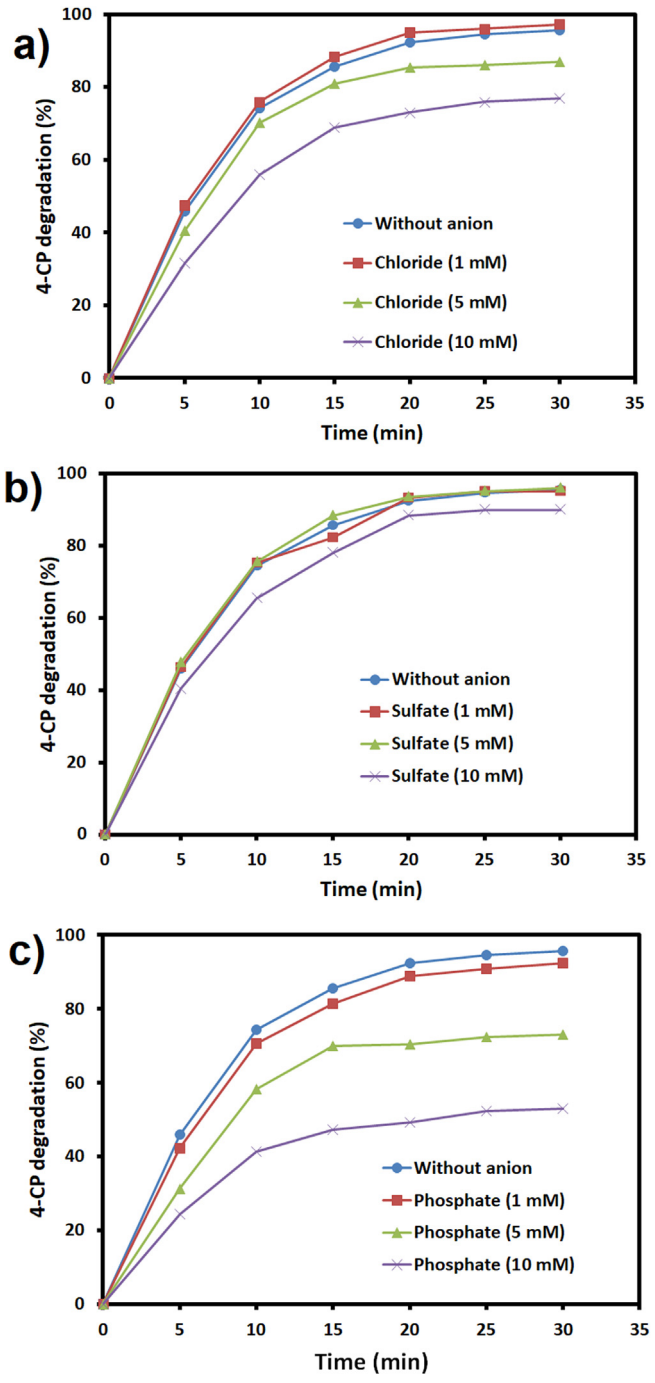

Fig. 7. the effect of anions on 4-CP degradation (a) chloride ion (b) sulfate ion (c) phosphate ion (nZVI = 0.4 g/L, PMS = 1.25 mM, pH = 3.0 and US power = 200 W).

3.7. Determining the reactive species

In US/PMS/nZVI system, both free radicals of sulfate and hydroxyl can participate in degradation of 4-CP. In order to determine the contribution of each free radical, classical quenching experiments were conducted by two alcohols. Ethanol (EtOH) with α-

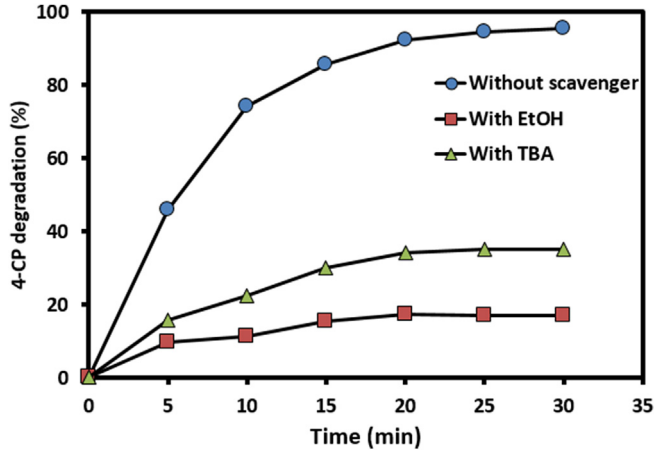

Fig. 8. the effect of EtOH and TBA (0.3 M) on 4-CP degradation (nZVI = 0.4 g/L, PMS = 1.25 mM, pH = 3.0 and US power = 200 W).

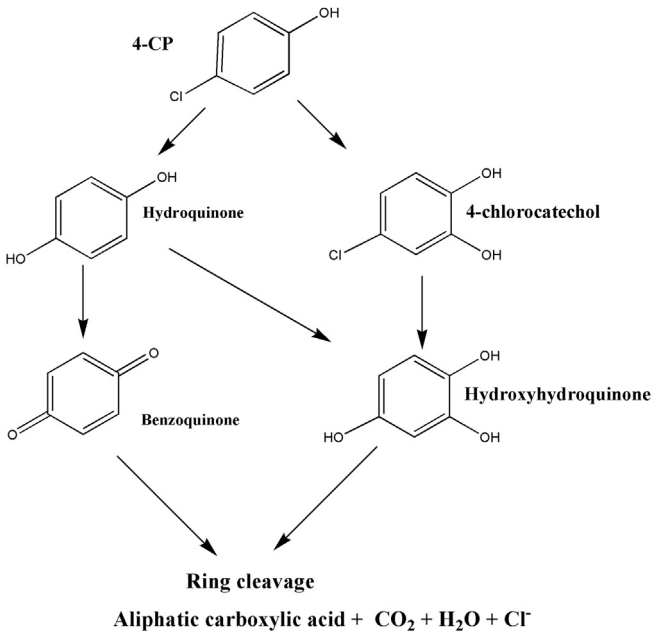

Fig. 9. Proposed pathway of 4-CP degradation by nZVI/PMS/US (nZVI = 0.4 g/L, PMS = 1.25 mM, pH = 3.0, US power = 200 W and 30 min).

hydrogen rapidly reacts with sulfate radical (the rate constant of $1.6–7.7 \times 10^7\ M^{-1}s^{-1}$) and hydroxyl radical (the rate constant of $1.2–2.8 \times 10^9\ M^{-1}s^{-1}$) while *tert*-butyl alcohol (TBA) is a specific scavenger for hydroxyl radical with the rate constant of $1.2–2.8 \times 10^9\ M^{-1}s^{-1}$ (Ghanbari and Moradi, 2017; Huang et al., 2017; Qi et al., 2013). On the other hand, the reactivity of TBA with sulfate radical is lower 1000 times less than that of EtOH. Fig. 8 shows the 4-CP degradation in the presence of TBA and EtOH (0.3 M) as scavenger. As can be seen, the 4-CP degradation efficiency was reduced from 95.6 to 35% in the presence of TBA, suggesting that the hydroxyl radical plays an important role for 4-CP degradation. While, compared to the condition with the presence of TBA, the degradation rate decreased limitedly in the presence of EtOH. These results showed that hydroxyl radical had more contribution in 4-CP degradation compared to sulfate radical. This phenomenon can related to the convert of sulfate radical to hydroxyl radical in the presence water molecule based on Eq. (14) (Lin et al., 2017).

$$SO_4^{\bullet-} + H_2O \rightarrow HO^{\bullet} + SO_4^{2-} + H^+ \quad (14)$$

Moreover, iron complex formed during reaction time can be a source of hydroxyl radical when US is irradiated into solution based on Eq. (15) (Ma, 2012).

$$[Fe(OH)]^{2+} + US \rightarrow Fe^{2+} + HO^{\bullet} \quad (15)$$

3.8. Reaction intermediates and the possible mechanistic pathway

The intermediates of 4-CP degradation were identified by LC-MS during 30 min reaction time. Mass-spectroscopy results are presents in Fig. S1. The proposed pathway of 4-CP degradation is presented in Fig. 9 based on formed intermediates during sono-oxidation. According to Fig. 9, 4-CP ($m/z = 128$) was hydroxylated and chlorine function was separated from 4-CP and hydroquinone ($m/z = 110$) was formed at the first step. After that, hydroquinone was oxidized to benzoquinone ($m/z = 108$) by free radicals. In another pathway, 4-CP was hydroxylated to 4-chlorocatechol ($m/z = 144$) with attack of hydroxyl radical. After that, chlorine function was eliminated from 4-chlorocatechol by free radicals, and hydroxyhydroquinone ($m/z = 126$) was formed. It should be noted that hydroquinone was also hydroxylated by free radicals and hydroxyhydroquinone was formed during sono-oxidation. Finally, the aromatic compounds of hydroxyhydroquinone and benzoquinone were opened and aliphatic carboxylic acids were produced consequently. Further oxidation of aliphatic carboxylic acids resulted in mineral compounds as final intermediates.

3.9. Application of US/PMS/nZVI for real petrochemical wastewater

The performance of US/PMS/nZVI was evaluated on real petrochemical wastewater and their results are presented in Table 1. As can be seen, COD, BOD and TOC were decreased during sonolysis time. COD was reduced from 1025 to 410 mg/L (60% removal efficiency) after 90 min while TOC was declined from 275 to 144 mg/L (47% removal efficiency) at the same reaction time. Total phenols were also eliminated from the wastewater with removal efficiency of 61%. BOD/COD value less than 0.3 is difficult to biodegradation while this value more than 0.4 is suitable for biological treatment (Jaafarzadeh et al., 2016; Kalyani et al., 2009). According to the results, BOD/COD of raw petrochemical wastewater was 0.24 indicating that this wastewater was persistence to biodegradation. After treatment with US/PMS/nZVI, BOD/COD value reached 0.41 illustrating that treated wastewater had been biodegradable. In other words, US/PMS/nZVI not only decreased organic content of real wastewater, but also it increased biodegradability of real wastewater. As shown in Table 1, TDS of the wastewater was increased after US/PMS/nZVI application. This increase is due to the presence of Oxone salt as source of PMS (Jaafarzadeh et al., 2016). Moreover, the release of ferrous ions also is another reason for increase of TDS. However, regarding the DI values obtained in Fig. 4, the release of Fe^{2+} is negligible for increase of TDS.

4. Conclusions

In this work, 4-CP was degraded by US/PMS/nZVI process. Under the optimum condition (pH = 3.0, nZVI = 0.4 g/L, PMS = 1.25 mM, US power = 200 W), 95% of 4-CP was removed during 30 min with rate constant of 0.1159 min^{-1}. nZVI had higher catalytic performance compared to mZVI, ferrous and ferric ions. Chloride exhibited a dual role in US/PMS/nZVI process in which high and low

Table 1
The performance of US/PMS/nZVI on real petrochemical wastewater during reaction time.

Parameters	Before treatment	After 30 min	After 60 min	After 90 min
COD (mg/L)	1025	750	575	410
BOD_5 (mg/L)	250	180	160	170
TOC (mg/L)	275	210	167	144
Total phenols (mg/L)	47.6	34.3	22.3	17.7
TDS (mg/L)	1185	1410	1440	1400
BOD_5/COD	0.24	0.24	0.27	0.41

concentration of chloride ions had negative and positive effects on 4-CP degradation respectively. Phosphate ions depicted high inhibitory effect on the performance of US/PMS/nZVI process. Scavenging experiments indicated that hydroxyl radical was dominant agent for 4-CP degradation. Intermediates of 4-CP degradation were also determined by LC-MS and proposed reaction for 4-CP degradation was illustrated. The performance of US/PMS/nZVI process for real petrochemical wastewater indicated that US/PMS/nZVI process can be a pretreatment for further biological process.

Acknowledgment

This research project has been financially supported by Behbahan Faculty of Medical Sciences (Grant No. 9625).

Appendix A. Supplementary data

Supplementary data related to this article can be found at https://doi.org/10.1016/j.chemosphere.2018.02.143.

References

Adewuyi, Y.G., 2005a. Sonochemistry in environmental remediation. 1. Combinative and hybrid sonophotochemical oxidation processes for the treatment of pollutants in water. Environ. Sci. Technol. 39, 3409–3420.
Adewuyi, Y.G., 2005b. Sonochemistry in environmental remediation. 2. Heterogeneous sonophotocatalytic oxidation processes for the treatment of pollutants in water. Environ. Sci. Technol. 39, 8557–8570.
Ahmadi, M., Ghanbari, F., Alvarez, A., Martinez, S.S., 2017. UV-LEDs assisted peroxymonosulfate/Fe2+ for oxidative removal of carmoisine: the effect of chloride ion. Kor. J. Chem. Eng. 34, 2154–2161.
Anipsitakis, G.P., Dionysiou, D.D., 2004. Radical generation by the interaction of transition metals with common oxidants. Environ. Sci. Technol. 38, 3705–3712.
APHA, 1999. Standard Methods for the Examination of Water and Wastewater, twentieth ed. APHA, Washington DC.
Babuponnusami, A., Muthukumar, K., 2012. Removal of phenol by heterogenous photo electro Fenton-like process using nano-zero valent iron. Separ. Purif. Technol. 98, 130–135.
Burbano, A.A., Dionysiou, D.D., Suidan, M.T., Richardson, T.L., 2005. Oxidation kinetics and effect of pH on the degradation of MTBE with Fenton reagent. Water Res. 39, 107–118.
Chan, K.H., Chu, W., 2009. Degradation of atrazine by cobalt-mediated activation of peroxymonosulfate: different cobalt counteranions in homogenous process and cobalt oxide catalysts in photolytic heterogeneous process. Water Res. 43, 2513–2521.
Czaplicka, M., 2004. Sources and transformations of chlorophenols in the natural environment. Sci. Total Environ. 322, 21–39.
Devlin, J.F., Allin, K.O., 2005. Major anion effects on the kinetics and reactivity of granular iron in glass-encased magnet batch reactor experiments. Environ. Sci. Technol. 39, 1868–1874.
Dong, H., He, Q., Zeng, G., Tang, L., Zhang, L., Xie, Y., Zeng, Y., Zhao, F., 2017. Degradation of trichloroethene by nanoscale zero-valent iron (nZVI) and nZVI activated persulfate in the absence and presence of EDTA. Chem. Eng. J. 316, 410–418.
Elghniji, K., Salem, S., Mosbah, M.b., Elaloui, E., Moussaoui, Y., 2014. Detoxification of 4-chlorophenol in TiO2 sunlight system: effect of raw and treated solution on seed germination and plants growth of various sensitive vegetables. Toxicol. Environ. Chem. 96, 869–879.
Ghanbari, F., Moradi, M., 2017. Application of peroxymonosulfate and its activation methods for degradation of environmental organic pollutants. Chem. Eng. J. 310, 41–62.
He, X., Armah, A., Dionysiou, D.D., 2013. Destruction of cyanobacterial toxin cylindrospermopsin by hydroxyl radicals and sulfate radicals using UV-254nm activation of hydrogen peroxide, persulfate and peroxymonosulfate. J. Photochem. Photobiol., A 251, 160–166.
Hernandez, R., Zappi, M., Kuo, C.-H., 2004. Chloride effect on TNT degradation by zerovalent iron or zinc during water treatment. Environ. Sci. Technol. 38, 5157–5163.
Huang, Q., Zhang, J., He, Z., Shi, P., Qin, X., Yao, W., 2017. Direct fabrication of lamellar self-supporting Co 3 O 4/N/C peroxymonosulfate activation catalysts for effective aniline degradation. Chem. Eng. J. 313, 1088–1098.
Hussain, I., Zhang, Y., Huang, S., Du, X., 2012. Degradation of p-chloroaniline by persulfate activated with zero-valent iron. Chem. Eng. J. 203, 269–276.
Jaafarzadeh, N., Ghanbari, F., Ahmadi, M., 2017. Efficient degradation of 2, 4-dichlorophenoxyacetic acid by peroxymonosulfate/magnetic copper ferrite nanoparticles/ozone: a novel combination of advanced oxidation processes. Chem. Eng. J. 320, 436–447.
Jaafarzadeh, N., Omidinasab, M., Ghanbari, F., 2016. Combined electrocoagulation and UV-based sulfate radical oxidation processes for treatment of pulp and paper wastewater. Process Saf. Environ. Protect. 102, 462–472.
Johnson, S.K., Houk, L.L., Feng, J., Houk, R., Johnson, D.C., 1999. Electrochemical incineration of 4-chlorophenol and the identification of products and intermediates by mass spectrometry. Environ. Sci. Technol. 33, 2638–2644.
Kalyani, K.S.P., Balasubramanian, N., Srinivasakannan, C., 2009. Decolorization and COD reduction of paper industrial effluent using electro-coagulation. Chem. Eng. J. 151, 97–104.
Lettmann, C., Hildenbrand, K., Kisch, H., Macyk, W., Maier, W.F., 2001. Visible light photodegradation of 4-chlorophenol with a coke-containing titanium dioxide photocatalyst. Appl. Catal., B 32, 215–227.
Li, R., Jin, X., Megharaj, M., Naidu, R., Chen, Z., 2015. Heterogeneous Fenton oxidation of 2, 4-dichlorophenol using iron-based nanoparticles and persulfate system. Chem. Eng. J. 264, 587–594.
Lin, X., Ma, Y., Wan, J., Wang, Y., 2017. LiCoPO 4 (LCP) as an effective peroxymonosulfate activator for degradation of diethyl phthalate in aqueous solution without controlling pH: efficiency, stability and mechanism. Chem. Eng. J. 315, 304–314.
Ling, S.K., Wang, S., Peng, Y., 2010. Oxidative degradation of dyes in water using Co 2+/H 2 O 2 and Co 2+/peroxymonosulfate. J. Hazard Mater. 178, 385–389.
Liou, Y.H., Lo, S.-L., Kuan, W.H., Lin, C.-J., Weng, S.C., 2006. Effect of precursor concentration on the characteristics of nanoscale zerovalent iron and its reactivity of nitrate. Water Res. 40, 2485–2492.
Ma, Y.-S., 2012. Short review: current trends and future challenges in the application of sono-Fenton oxidation for wastewater treatment. Sustain. Environ. Res. 22, 271–278.
Mahamuni, N.N., Adewuyi, Y.G., 2010. Advanced oxidation processes (AOPs) involving ultrasound for waste water treatment: a review with emphasis on cost estimation. Ultrason. Sonochem. 17, 990–1003.
Moonsiri, M., Rangsunvigit, P., Chavadej, S., Gulari, E., 2004. Effects of Pt and Ag on the photocatalytic degradation of 4-chlorophenol and its by-products. Chem. Eng. J. 97, 241–248.
Neta, P., Huie, R.E., Ross, A.B., 1988. Rate constants for reactions of inorganic radicals in aqueous solution. J. Phys. Chem. Ref. Data 17, 1027–1284.
Pan, X., Yan, L., Li, C., Qu, R., Wang, Z., 2017. Degradation of UV-filter benzophenone-3 in aqueous solution using persulfate catalyzed by cobalt ferrite. Chem. Eng. J. 326, 1197–1209.
Qi, F., Chu, W., Xu, B., 2013. Catalytic degradation of caffeine in aqueous solutions by cobalt-MCM41 activation of peroxymonosulfate. Appl. Catal., B 134, 324–332.
Qi, F., Chu, W., Xu, B., 2014. Modeling the heterogeneous peroxymonosulfate/Co-MCM41 process for the degradation of caffeine and the study of influence of cobalt sources. Chem. Eng. J. 235, 10–18.
Sauleda, R., Brillas, E., 2001. Mineralization of aniline and 4-chlorophenol in acidic solution by ozonation catalyzed with Fe 2+ and UVA light. Appl. Catal., B 29, 135–145.
Su, S., Guo, W., Yi, C., Leng, Y., Ma, Z., 2012. Degradation of amoxicillin in aqueous solution using sulphate radicals under ultrasound irradiation. Ultrason. Sonochem. 19, 469–474.
Sun, H., Kwan, C., Suvorova, A., Ang, H.M., Tadé, M.O., Wang, S., 2014. Catalytic oxidation of organic pollutants on pristine and surface nitrogen-modified carbon nanotubes with sulfate radicals. Appl. Catal., B 154, 134–141.
Taha, M.R., Ibrahim, A.H., 2014. Characterization of nano zero-valent iron (nZVI) and its application in sono-Fenton process to remove COD in palm oil mill effluent. J. Environ. Chem. Eng 2, 1–8.
Theurich, J., Lindner, M., Bahnemann, D., 1996. Photocatalytic degradation of 4-chlorophenol in aerated aqueous titanium dioxide suspensions: a kinetic and mechanistic study. Langmuir 12, 6368–6376.
Tong, Z., Qingxiang, Z., Hui, H., Qin, L., Yi, Z., 1997. Removal of toxic phenol and 4-chlorophenol from waste water by horseradish peroxidase. Chemosphere 34, 893–903.
Vilar, V.J.P., Amorim, C.C., Brillas, E., Puma, G.L., Malato, S., Dionysiou, D.D., 2017. AOPs: recent advances to overcome barriers in the treatment of water, wastewater and air. Environ. Sci. Pollut. Res. 24, 5987–5990.
Vogel, A.I., 1989. Vogel's Textbook of Quantitative Chemical. Longman Scientic & Technical, London.
Wang, C.-B., Zhang, W.-X., 1997. Synthesizing nanoscale iron particles for rapid and complete dechlorination of TCE and PCBs. Environ. Sci. Technol. 31, 2154–2156.
Wang, P., Yang, S., Shan, L., Niu, R., Shao, X., 2011. Involvements of chloride ion in decolorization of Acid Orange 7 by activated peroxydisulfate or peroxymonosulfate oxidation. J. Environ. Sci. 23, 1799–1807.
Wang, Y., Chu, W., 2012. Photo-assisted degradation of 2, 4, 5-trichlorophenoxyacetic acid by Fe (II)-catalyzed activation of Oxone process: the role of UV irradiation, reaction mechanism and mineralization. Appl. Catal., B 123, 151–161.
Wilfert, P., Kumar, P.S., Korving, L., Witkamp, G.-J., van Loosdrecht, M.C., 2015. The relevance of phosphorus and iron chemistry to the recovery of phosphorus from wastewater: a review. Environ. Sci. Technol. 49, 9400–9414.
Xu, L., Wang, J., 2011. A heterogeneous Fenton-like system with nanoparticulate zero-valent iron for removal of 4-chloro-3-methyl phenol. J. Hazard Mater. 186, 256–264.
Yao, J., Zeng, X., Wang, Z., 2017. Enhanced degradation performance of sulfisoxazole using peroxymonosulfate activated by copper-cobalt oxides in aqueous solution: kinetic study and products identification. Chem. Eng. J. 330, 345–354.
Yazdanbakhsh, A., Mehdipour, F., Eslami, A., Maleksari, H.S., Ghanbari, F., 2015. The

combination of coagulation, acid cracking and Fenton-like processes for olive oil mill wastewater treatment: phytotoxicity reduction and biodegradability augmentation. Water Sci. Technol. 71, 1097–1105.
Yuan, N., Zhang, G., Guo, S., Wan, Z., 2016. Enhanced ultrasound-assisted degradation of methyl orange and metronidazole by rectorite-supported nanoscale zero-valent iron. Ultrason. Sonochem. 28, 62–68.
Zha, S., Cheng, Y., Gao, Y., Chen, Z., Megharaj, M., Naidu, R., 2014. Nanoscale zero-valent iron as a catalyst for heterogeneous Fenton oxidation of amoxicillin. Chem. Eng. J. 255, 141–148.
Zhou, T., Li, Y., Ji, J., Wong, F.-S., Lu, X., 2008. Oxidation of 4-chlorophenol in a heterogeneous zero valent iron/H 2 O 2 Fenton-like system: kinetic, pathway and effect factors. Separ. Purif. Technol. 62, 551–558.
Zou, X., Zhou, T., Mao, J., Wu, X., 2014. Synergistic degradation of antibiotic sulfadiazine in a heterogeneous ultrasound-enhanced Fe0/persulfate Fenton-like system. Chem. Eng. J. 257, 36–44.